Journal of ELECTRONIC MATERIALS
DOI: 10.1007/s11664-016-4598-y


# Fabrication and Characterization of $TiO_2$ Nano Rods by Electrochemical Deposition into an Anodic Alumina Template

MUHAMMAD IKRAAM,[1] SAMMIA SHAHID,[1,3] SABAH ZAMAN,[2] and M.N. SARWAR[2]

1.—Department of Chemistry, School of Science, University of Management & Technology, Lahore 54770, Pakistan. 2.—Ibn-e-Sina Institute of Technology, Islamababd 44000, Pakistan. 3.—e-mail: drsammiashahid@gmail.com

Titanium dioxide ($TiO_2$) nanorods have been successfully grown into a track-etched anodized aluminium oxide membrane (AAM) by a particulate electrochemical deposition from an aqueous medium. The prepared $TiO_2$ sols get stabilized against aging at pH 2. It was found that $TiO_2$ nanorods grown from dilute aqueous solution with a low concentration gave a stable and uniform growth. X-ray diffraction (XRD) results revealed that $TiO_2$ nanorods dried at 500°C were a mixture of anatase and brookite phases. Atomic Force Microscope (AFM) images confirmed that $TiO_2$ nanorods had a smooth morphology and longitudinal uniformity in diameter. A scanning electron microscope (SEM) image showed that $TiO_2$ nanorods grown by electrochemical deposition from the dilute aqueous sol had a dense structure and possessed a repetitive pattern, containing small particles with an average size of 15 nm. Based on kinetic studies, it was found that uniform $TiO_2$ nanorods with high-quality morphology were obtained under optimum conditions at an applied potential of 5 V, a uniform current density of 500 mA, and a deposition time of 5 h.

**Key words:** $TiO_2$ nanorods, anodized aluminium oxide template, electrochemical deposition, kinetic studies

## INTRODUCTION

Titanium dioxide or Titania ($TiO_2$) is a well-known, chemically stable nontoxic transition-metal oxide, which has been extensively used in the pigment industry for several decades.[1] This material is also used in various novel applications and is known as an advanced material. It has been considered probably to be the most studied transition metal oxide owing to its many extraordinary physical, chemical, electronic, electrochemical, and photoactive properties.[2,3] $TiO_2$ has also attracted vast interest in chemical engineering related research including solar energy conversion through dye sensitized and quantum-dot-sensitized solid-state solar cells, water splitting, general photocatalysis, lithium ion batteries, super capacitors, chemical/gas sensing, controlled release, environmental remediation including indoor air purification, wastewater treatment, antifogging, self-cleaning, de-odoration, and deactivation of bacteria.[4,5] Titanium dioxide is both intrinsic and N-type (non-intentionally doped), due to oxygen vacancies in the $TiO_2$ lattice, its properties are similar to ZnO. Titanium dioxide displays N-type semiconducting properties at ambient temperature due to a tendency for oxygen deficiency, which manifests itself in the formation of either oxygen vacancies or titanium interstitials; both of which are donor type defects,[6] At elevated temperatures (greater than 1273 K), un-doped $TiO_2$ has demonstrated weak *P*-type behaviors in high oxygen activity, but no observation of room temperature *P*-type semiconductivity exists.[7] It is, in fact,

(Received February 10, 2016; accepted April 28, 2016)

Published online: 10 May 2016

the most commercially used metal oxide semiconductor material because of its excellent mechanical and chemical stability and the rather low cost. Due to inertness and resistant to chemical and sunlight corrosion, $TiO_2$ devices can be used for long periods of time at ambient conditions.[8,9] In addition, $TiO_2$ nanostructures are highly resistant to organic solvents, and have high electron–hole recombination times, compared to the other metal oxide semiconductors, which are desirable in photocatalytic decomposition of organic materials.[10] They also have strong oxidizing power from the generated holes and redox selectivity.[11] Synthesis of one-dimensional nanostructure such as nanotubes and nanorods is usually considered because of their supreme capabilities in photoelectrochemical reactions due to their improved charge transfer.[12] Over the past few years, nanoporous $TiO_2$ structures have also been formed by electrochemical anodization of titanium.[13] This method has been also proposed for several advantages and applications.[14] $TiO_2$ nanorods are more biocompatible, non-toxic, and environmentally friendly due to larger surface area as compared with nanoparticles.[15] They can be used for controlled catalysis,[16] photonic crystals,[17] wave guides,[18] and reflectors.[19]

$TiO_2$ nanorods and nanofibers have been developed using different techniques, such as sol–gel template processing,[20] electro-deposition template processing[21] and anodization.[22,23] Among various methods of processing of nanostructure metal oxides; anodization is considered to be the most effective for obtaining nanoporous or nanotubular structures. Anodized aluminium oxide (AAO), also known as aluminais, is one of the most studied nanoporous materials, having a self-ordered porous structure. Anodized aluminium oxide obtained by anodization has been investigated for several decades, and the optimal conditions have been established.[24] In this method, $TiO_2$ nano-architectures, such as nanorods, were grown in the nanoholes of the anodized aluminum oxide (AAO) templates.[25,26] The template method possesses obvious advantages, such as simplicity, low cost, and low demand of raw materials and devices. However, it possesses many limitations such as the preparation process is very complex, the obtained nano-architectures depend entirely on the size and shape of the template and the post-treatment process of the templates tends to damage the morphologies of the nano-architectures. However, based on its extraordinary applications and properties, scientists are continuously trying to prepare the nanostructure in easier and a more commercial manner so that industrial applications can be feasible. In this research work we have also focused on the same effort. The main purpose of this research was to develop a low cost method by using approximately 98% pure Al metal, which is less expensive in comparison to highly pure (99.99%) Al-metal. Highly pure Al is very expensive and is commonly used for nanofabrication. Quite expensive platinum or gold as a counter inert electrode was replaced with the carbon rod as the inert electrode. An easyily attainable temperature 5–10°C was used, instead of temperatures 0–3°C, which may be achieved with ease. Titanium dioxide ($TiO_2$) powder was used, instead of titanium Isopropoxide or related chemicals, which are very expensive for nanofabrication. This synthesis was processed at ambient conditions instead of any inert or argon atmosphere, like most of the early narrated methods.[28]

## EXPERIMENTAL

The aluminium alloy sample was analyzed by SGS Pakistan Pvt. Ltd. The composition (wt.%) of the alloy was 0.37% zinc, 0.160% magnesium, 0.243% copper, 0.105% iron, 0.150% chromium, 0.111% silicon, 0.014% manganese, and aluminium in balance.

## TEMPLATE PREPARATION

A 2.75-mm thick aluminium sheet of 98.9% purity was used for the AAO template fabrication. The aluminium sheet was polished and cleaned with the help of sand paper having grade 1500 and 2000 to remove any corrosion and other hard impurities that may be found over its surface and then washed with copious distilled water and acetone to remove any remaining dust or dirt. The aluminium sheet was first annealed at 500°C for 23 h using a muffle furnace equipped with a continuous power supply. The purpose of the annealing was to get good grain size. The annealed sheet was electro-polished in a solution of sulphuric acid: phosphoric acid: deionized water having a ratio 2:2:3 to remove impurities and contaminants from the surface of the sheet and to convert it into a highly polished and clear surface. The electropolished sheet was then ready for anodization. An acid resistant tank was used for anodizing. For the first anodization of the Al, a constant voltage of 45 V was applied using a standard digital voltage regulator for 5 h in a 0.3 M oxalic acid solution maintained at 6–8°C. The overall setup of the process was as shown in Fig. 1.

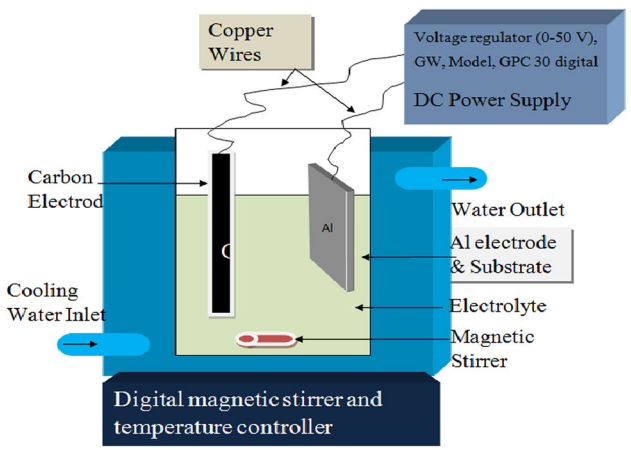


Fig. 1. Anodization process setup for pore generation and nanorods growth.

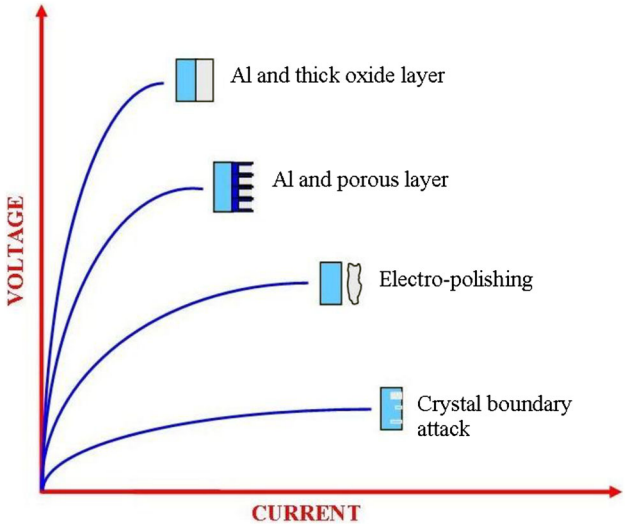


Fig. 2. Anodic polarization of aluminium in different electrolyte solutions.

This temperature was as the maximum possible temperature at which $TiO_2$ nanorods could be prepared commercially. The hexagonal pore arrangement was formed on porous anodic alumina at 6–8°C. Disordered porous anodic alumina is formed in oxalic acid at higher temperature. The temperature of the oxalic acid electrolyte effects the movements of ions in the electrolyte and across the barrier layer and heat dissipation within the porous anodic alumina during anodization. Voltage was critically important during this step as shown in Fig. 2. At very high voltage and at very low current only a thick oxide layer will be deposited, while at relatively lower voltage and higher current, a crystal boundary attack will result and irregular and defected pore growth occurrs. Hence, a very closed and optimum setting of voltage and current is required for this purpose.[27]

The temperature of the bath was continuously monitored. The aluminium sheet was immersed in the oxalic acid solution in an anodizing bath, placed in between the external water bath, which functioned as a temperature controller bath. The cathode was a carbon rod and an aluminium sheet was the anode. Both the electrodes were provided conducting contacts with an external DC power supply with the help of copper wires.

The grown alumina layer with pores was etched away in a solution of a mixture of phosphoric acid (6 wt.%) and chromic acid (1.8 wt.%) at 60°C. The temperature of the system was monitored using a digitally controlled hot plate with buil in stirring and temperature control options. The etching and removing of the grown alumina layer left behind a clear pattern for a regular growth of the second anodization as shown in Fig. 3.

The second anodization to obtain a regular array of nanochannels was carried out for 5 h under the same conditions, applied for the first anodization.

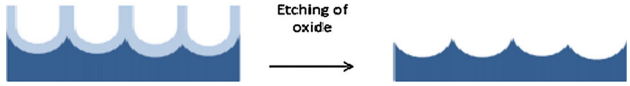


Fig. 3. Removal of oxide after an initial anodization the aluminium surface is structured.

The pores in alumina were then widened by etching in 0.1 M phosphoric acid for 40 min at 40°C. After the anodization process, un-reacted aluminium (Al) was removed in 1 M phosphoric acid for 3–5 min or in 0.2 M $HgCl_2$ by immersing the alumina grown sheet in it for 2–3 min at ambient temperature. The barrier layer was removed with 1 M phosphoric acid at ambient temperature.[28] The net chemical equation that resulted after the anodization is very simple, and it is understandable that an Al substrate and an exacting acid were used to get nanopores having an empirically derived set of the electrochemical environment.

$$\text{Aluminium} + \text{acid} + \text{voltage} \rightarrow \text{nano-pores}$$

## NANORODS DEPOSITION PROCESS

The titanium dioxide ($TiO_2$) colloidal suspension was prepared by dissolving 4.14 g of titanium dioxide powder into 300 ml of distilled water and stirring for 30 min at room temperature. Then glacial acetic acid was mixed with deionized water with continuous stirring followed by sonication for 30 min to dissolve the maximum possible amount of titanium dioxide. The resulting white suspension was used as a depositing substrate.

The titanium dioxide nanorods were grown on an alumina template at 25–30°C. An anodized aluminium sheet was dipped into the prepared colloidal suspension of titanium dioxide. For the electrophoretic deposition, a carbon rod was used as the anode, and an AAM was used as the cathode. The pH of the colloidal suspension was maintained at 2–3 with the help of a small amount of nitrate acid. Titanium dioxide has good stability against aging at pH 2. This colloidal suspension was stable at low pH.[29] The deposition was kept continually for 2 h by keeping the voltage at 3–5 V and the current density at 500 mA. Higher voltage and current density could cause rapid and irregular deposition. After the completion of the deposition, the anodized aluminium substrate was kept out of the suspension, washed with plenty of distilled water and dried at 80°C. In order to crystallize the attained anodic oxide nanostructured layers, following anodization, samples were thermally annealed in a furnace at temperatures 450–500°C in air.

The template was removed by immersion into a 3 M NaOH solution for 5 min to partly dissolve the template membrane and dried at 80°C for 2 h. Here again the net equation that resulted after the deposition was very simple and understandable, i.e.,

The overall process could be summarized as:

$$\text{Aluminium} + \text{acid} + \text{voltage} \rightarrow \text{nano-pores}$$

$$\text{Nano}-\text{pores} + \text{Colloidal suspension} + \text{current} \rightarrow \text{nanorods}.$$

## CHARACTERIZATION TECHNIQUES

The structural properties of $TiO_2$ nanorods were analyzed by x-ray diffraction (XRD, PanalytiCalX'Pert Pro) using Cu K$\alpha$ radiation ($\lambda$ = 1.54056 Å) at 40 kV and 30 mA. The surface morphologies were investigated by scanning electron microscopy (SEM, Jeol, 5910LV) and atomic force microscopy (AFM, Shimadzu-SPM-9500J3)

## RESULTS AND DISCUSSION

### Alumina Template

The porous alumina film was developed by applying the anodization process to Al and by keeping the current and voltage stable. For the growth of the required pores diameter, the steady form of the voltage is necessary.

Two-step anodization results in a uniform sized template for nanorod growth. The production of alumina in the first anodization on the exterior surface of the aluminium sheet was different than the second anodization. The effect of current and voltage on the growth of the alumina template against time $T$ was studied as shown in Figs. 4 and 5.

These graphs indicate the variation in the set parameters and effect on anodization with respect to time. During the first anodization, even a very little current produces a sufficient and large effect on the anodization, but after passage ofa little time of up to 4–5 min, its effect get stabilized on the sheet due to the start-up of the oxide development process on the Al surface. Similarly, the increase of the voltage was also very much slower during the first anodization up to 17 s, and then it gets stabilized during both anodization steps. These variations in current and voltage are traceable and linear without any significant error if controlled properly and not letting them deviate for a long period. It depends on many factors including bath temperature, electrolyte used, purity of the aluminium sheet, and counter electrode. During working, it was observed that the voltage declined by raising the temperature, and this is not a direct effect on voltage. The effect of temperature on voltage is an indirect effect, which is associated with other properties of the material (electrode and electrolyte, which changes accordingly with the temperature. Here, we include stumpy temperatures of the electrolyte and an out of the ordinary chemical composition of electrolyte. In addition, in this study – the boost in the electrolyte temperature directs to a slow diminution in the nanoholes value. A more considerable reduction in the nano holes takes place when using inferior values of the current density.[30] The

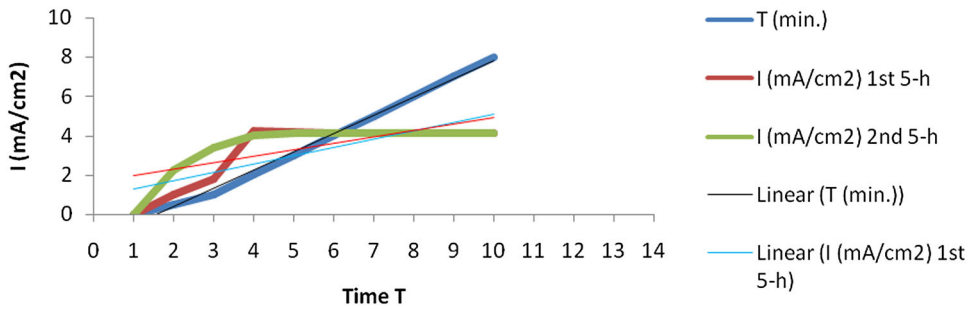


Fig. 4. Effect of current ($I$) versus time ($T$) on the anodization. The voltage and temperature were kept constant at 45 V and 6–8°C, respectively (Color figure online).

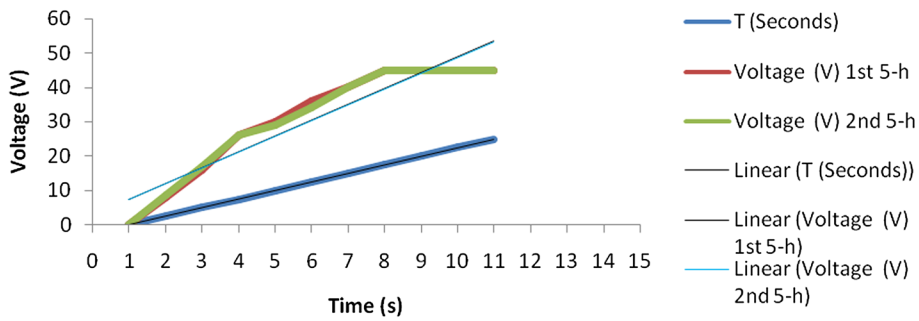


Fig. 5. Effect of voltage (V) versus time (s) on the anodization at 6–8°C (Color figure online).

surface of the alumina (treated) does not swell in a significant way as does by the flat sheet of the alumina. Therefore, a uniform layer of the alumina was created at ambient temperatures. The layer of the oxide formed as a result of anodization and was thinnest at the bottom of the each pore. Pore growth was lower and irregular when the applied current was higher, and the pore growth occurred only on the top surface instead of going into the depth. Such a template results in a very short range of nanorods with an irregular pattern. Hence, for better and deep growth, a small amount of current was used to produce a higher effect without overshooting the current[31,32] as given in Tables I and II.

## Structural Properties of $Tio_2$ Nanorods

The XRD analysis indicated that the prepared nanorods were a mixture of anatase and rutile phases as given in Fig. 6. Measurements of XRD of $TiO_2$ usually exist in two main crystallographic forms, anatase (A) and rutile (R). The XRD peaks at 2 h = 25.3° (101) and 2 h = 27.4° (110) are often taken as the characteristic peaks of the anatase and rutile crystal phase, respectively. The crystallite size can be determined from the broadening of corresponding x-ray spectral peak by Scherrer's formula

$$\tau = \frac{k\lambda}{\beta \cos\theta},$$

where $\tau$ is the crystallite size, $K$ is the wavelength of the x-ray radiation (in our test = 0.15406 nm), $K$ is usually taken as 0.89, and $\beta$ is the full width at half-maximum height of the main intensity peak after subtraction of the equipment broadening. Meanwhile, the percentage of anatase in the $TiO_2$ samples can also be estimated from the respective integrated characteristic XRD peak intensities using the quality factor ratio of anatase to rutile (1.265). The detailed XRD pattern of the $TiO_2$ nano structures is given in Fig. 5. The XRD pattern reveals peaks arising from $2\theta$ values of 39.67° (111), 40.24° (101), and 44.15° (210) that were well indexed to rutile $TiO_2$ (JCPDS card no. 761940) and peaks at 37.95° (004) and 64.5° (211) as anatase $TiO_2$ (JCPDS card no. 211272). The XRD spectra reveal that the sample consists of $TiO_2$ nanorods in both anatase and rutile phase. None of the alumina or other peaks was detected in an XRD pattern. The FWHM of all the peaks is quite narrow, suggesting the fine crystallinity in the synthesized $TiO_2$ nanorods.

**Table I. Effect of current (I) and time (T) on the anodization in 0.3 M oxalic acid**

| Time (*T* in min) | Current (I in mA/cm$^2$) in first 5-h | Current (I in mA/cm$^2$) in second 5-h |
|---|---|---|
| 0 | 0 | 0 |
| 0.5 | 1 | 2.25 |
| 1 | 1.8 | 3.4 |
| 2 | 4.25 | 4 |
| 3 | 4.2 | 4.15 |
| 4 | 4.15 | 4.12 |
| 5 | 4.14 | 4.12 |
| 6 | 4.13 | 4.12 |
| 7 | 4.13 | 4.12 |
| 8 | 4.13 | 4.12 |

The voltage and temperature was kept at 45 V and 6–8°C, respectively.

**Table II. Effect of voltage (V) and time (T) in 0.3 M oxalic acid**

| Time (s) | Voltage (V) first 5-h | Voltage (V) second 5-h |
|---|---|---|
| 0 | 0 | 0 |
| 2.5 | 8 | 8.5 |
| 5 | 16 | 17 |
| 7.5 | 26 | 26 |
| 10 | 30 | 29 |
| 12.5 | 36 | 34 |
| 15 | 40 | 40 |
| 17.5 | 45 | 45 |
| 20 | 45 | 45 |
| 22.5 | 45 | 45 |

The temperature was kept constant at 6–8°C, respectively.

## Morphological Properties

SEM images of an anodized alumina template at various nanometer ranges are given in Fig. 7a–d. The ideal pores of the hexagonal array of very good quality are obtained when anodization was carried

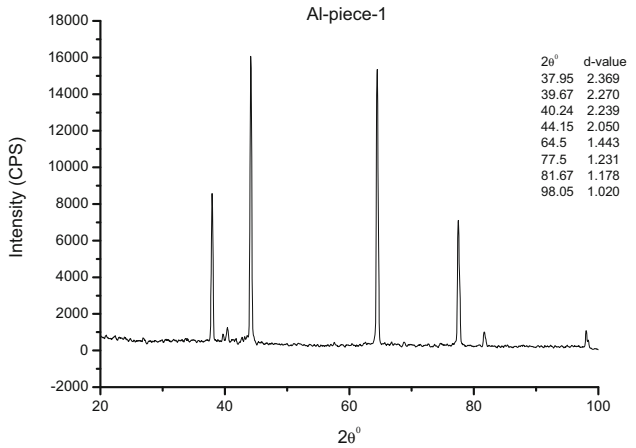


Fig. 6. The XRD spectra of the $TiO_2$ nanostructures synthesized via two-step anodization.

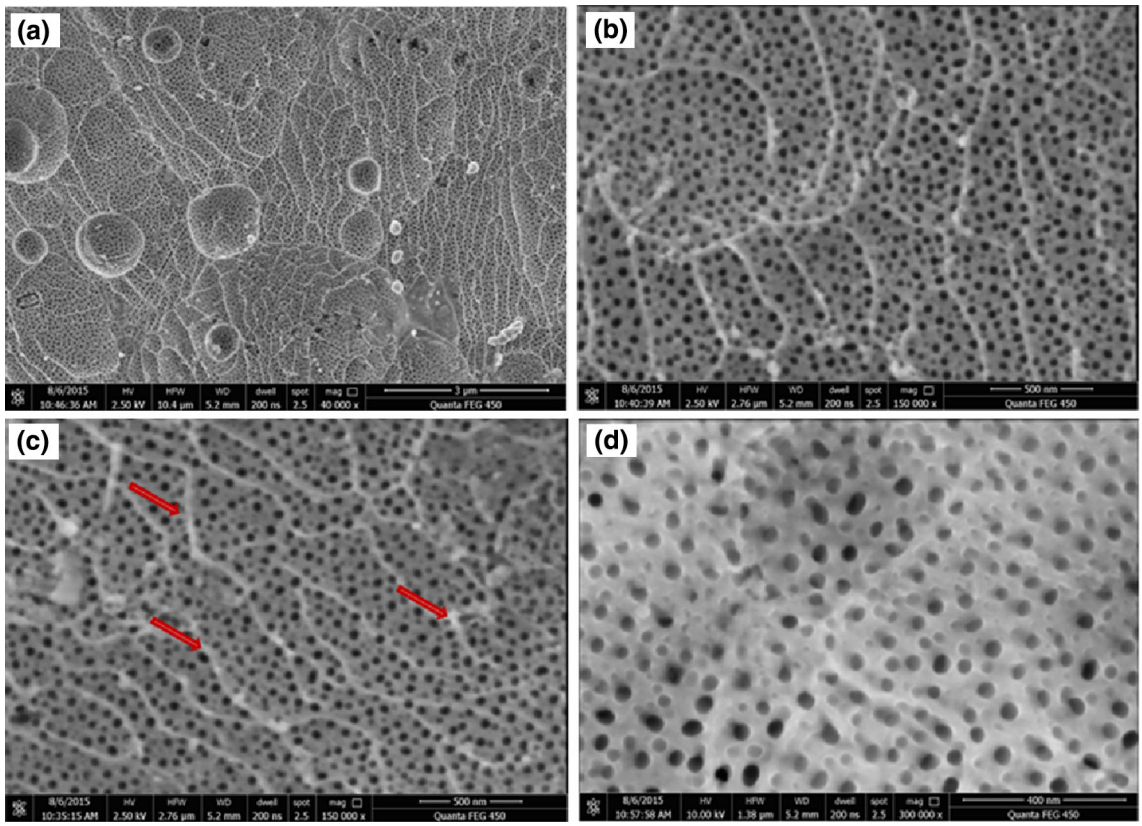


Fig. 7. SEM images of aluminium oxide template (AAO) prepared in 0.3 M. $H_2C_2O_4$ at 45 V top (a) 3 $\mu$m, (b) 500 nm and bottom (c) 500 nm, (d) 400 nm.

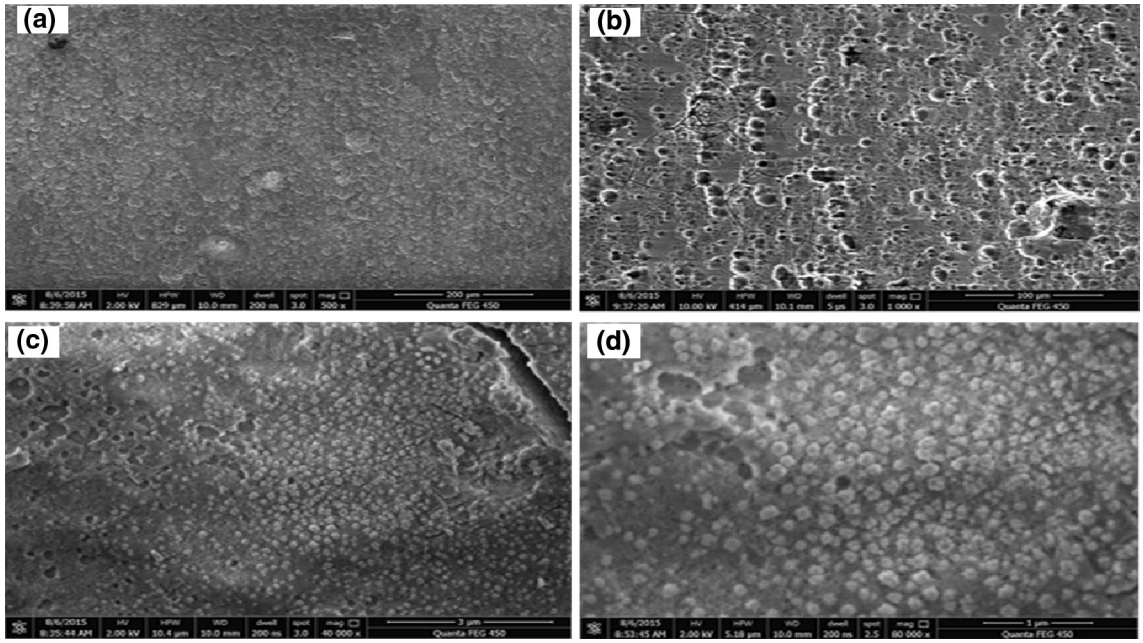


Fig. 8. SEM images of $TiO_2$ nanorods showing coalescence behaviour (a) 200 $\mu$m, (b) 100 $\mu$m, (c) 3 $\mu$m, and (d) 1 $\mu$m.

out for a longer time. These pores are of the alumina whose anodization was processed for 5 h. During this procedure, a chexagonal and densely packed array of a straight and parallel nature shifted from the interface of metal oxide to oxide electrolyte. The microscopic nanostructures encouraged the use of

AAO templates for the production and development of the nanostructure-based devices and materials. The benefit of the two-step anodization is the production of a good quality textured layer of the oxide, especially during the second or third anodization.[33]

After the first and second anodization, the layer of the oxide should be stripped off. At low magnification (Fig. 7a and b), this ordered structure shows domain structures. These domain structures are time dependent. These domain structures continue growing during anodization. However, in case of impurities in the aluminium template or random variations in set conditions, defects in domain structure could occur. The two most commonly known defects are the point defects and the misfit dislocations. It could be seen that there are some large "islands" (point defects), in the domain and each "island" has been surrounded by neighboring pores (Fig. 7a). On the other hand, the misfit dislocation of the pores line also interrupted the periodic arrangement of the pores (Fig. 7c). Materials with plenty of such defects seriously limit their technical applications, for the most part, in optoelectronic devices due to the interruption of their operation based on the electron and hole transfer mechanism. It is expected these shortcomings could be overcome by further optimizing the growth conditions.[34]

Figure 8a–d represents the surface morphology of $TiO_2$ nanorods grown in the alumina template. These scans were taken after the removal of the template. It should be noted that $TiO_2$ growth is continued by means of oriented coalescence of the primary created $TiO_2$ nanorods since they were established by many side-by-side aggregated $TiO_2$ (Fig. 8a–d) and resulted in the instantaneous enlargement of width and length of $TiO_2$. The droplet collision and coalescence can be prevented by the addition of the surfactant into the electrolyte; so it should be noted that the system should be kept free of such contaminations. Such coalescence of the nanoparticles on substrates shows an outcome in the development of very uniform and well-ordered nanorods.

## One-Dimensional (1-D) Nanostructures

Figure 9 represens the $TiO_2$ nanorod image produced by $TiO_2$ taken from a commercially available powder of titanium dioxide.

The SEM images of $TiO_2$ nanorods in Figs. 7 and 8 confirm that the produced nanorods via anodization are continuous, dense, and a repeatable composite. It can be seen that these exhibited fine rods-

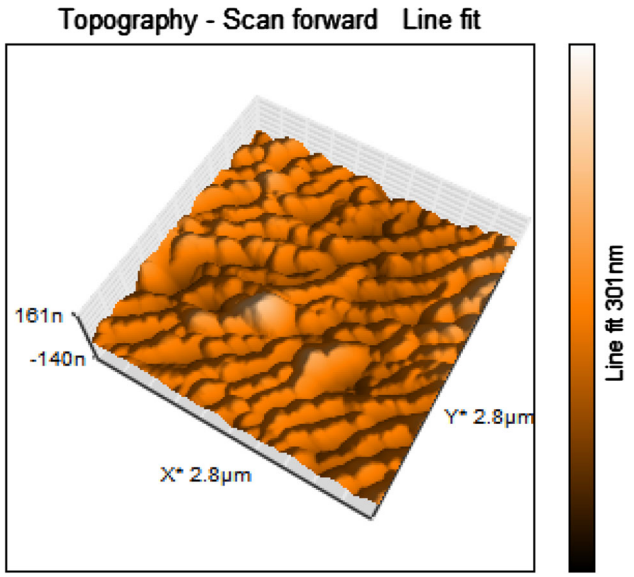


Fig. 10. Three-dimentional AFM image of $TiO_2$ nanorods (Color figure online).

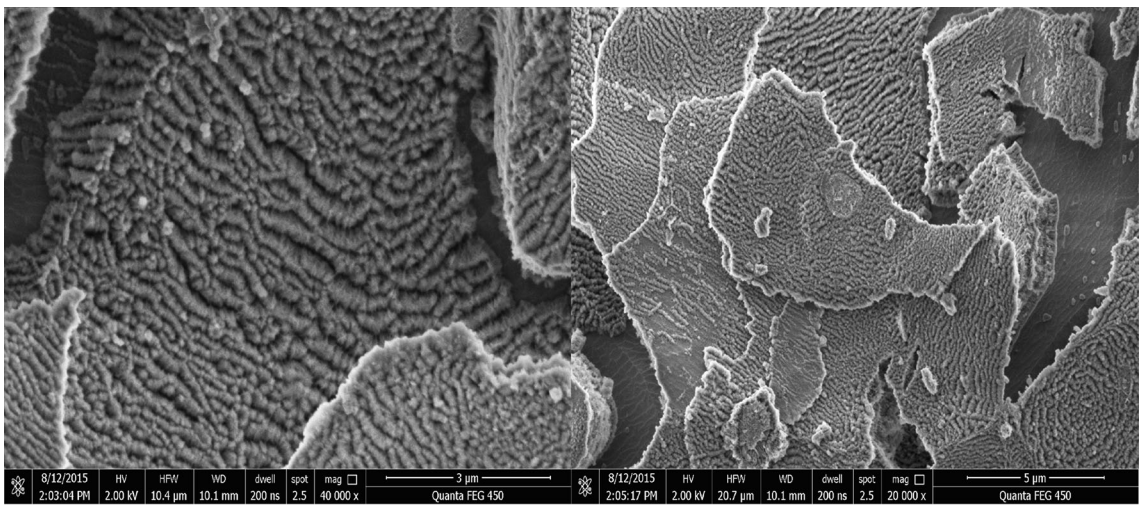


Fig. 9. SEM cross sectional image of the $TiO_2$ nanorods obtained after two-step anodization of the aluminium and removal of template.

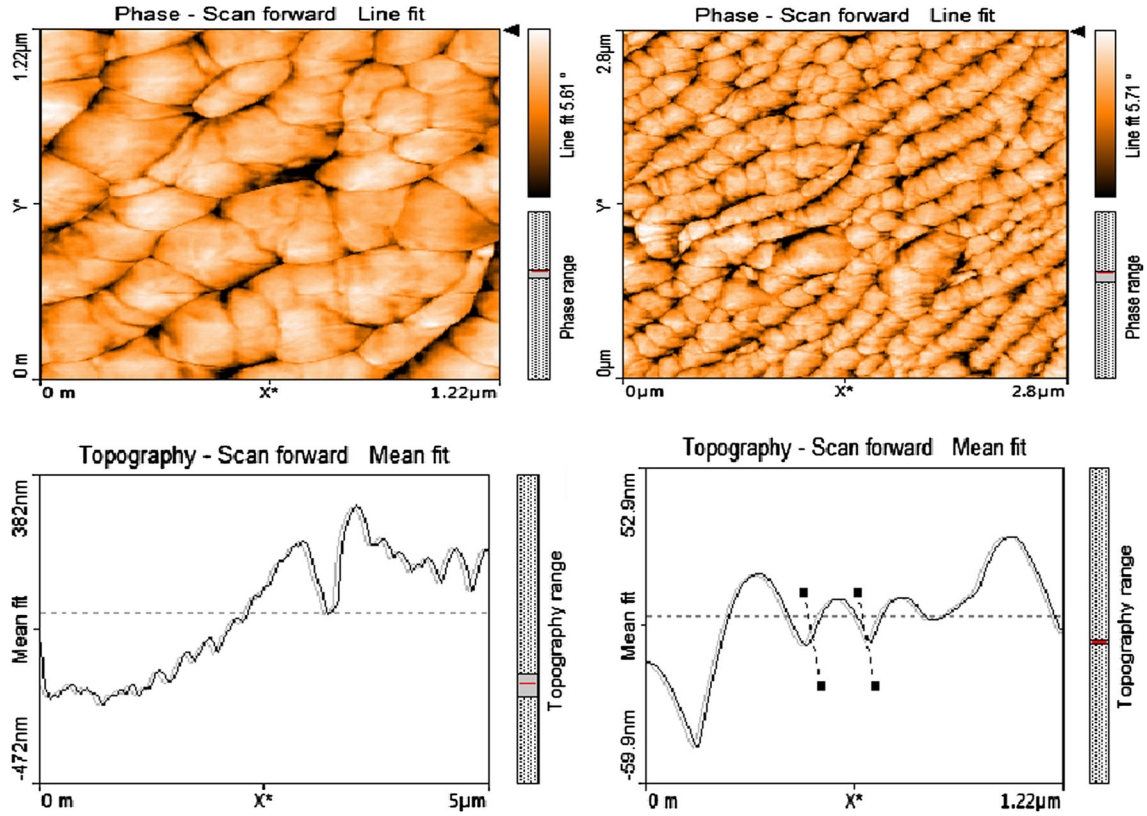


Fig. 11. AFM images of $TiO_2$ nanorods (Color figure online).

like morphologies and highly ordered structures. So $TiO_2$ nanorods were successfully deposited on the inner surface of the anodized alumina.

### Afm Images of Ordered Pores

The topographical study and nanomechanical properties of nanorods were studied using atomic force microscope (AFM). Images taking by AFM indicated the average width and length of $TiO_2$ nanorods to be 42 nm and 84 nm, respectively. The AFM images of $TiO_2$ nanorods are given in Figs. 10 and 11. The features of the nanorods at micro and nano-scale can be experimental, depicting the uniform and smooth growth of the material. The image space is $(x,y) = (2.80\ \mu m \times 2.80\ \mu m)$ in $A$ and $(x,y) = (1.2\ \mu m \times 1.2\ \mu m)$ in $B$.

Figure 11 shows the surface morphology of the prepared nanorods, which clearly indicates nanorods and their aggregation. Densely assembled and unidirectionally arranged nanorods with diameters 40 nm to 90 nm and lengths of several micrometers are observed. The diameter of these nanorods is almost fitting the diameter of the alumina template.

## CONCLUSION

A wel- ordered AAO template was successfully prepared via anodizing an Al sheet. This is a more cost effective process than those utilizing 99.99% Al. This could be achieved when a constant voltage was applied during anodization. It has been also observed that at the same time some key parameters affect the development process and rate of growth of a porous oxide layer. These parameters included anodization voltage, electrolyte composition, and temperature. These basic parameters also have an effect on interpore spacing in AAO template formation; during the first anodization, the time of anodization also has a very strong and powerful effect on the order-arrangement of pore arrays on an AAO-prepared template. Similarly, just as done previously and in order to sustain the same AAO templates developed in 0.3 M oxalic acid and with similar conditions applied for anodization for the two-step process of anodization, the diameters of the developed pores could be well-controlled in the ordered range of up to 25–93 nm. However, the temperature for this activity is kept low and the pore is possibly widened and adjusted by the application of phosphorus acid solution at 5 wt.% concentration. Ordered AAO templates with variable pore dimensions and diameters are the result of this setup. However, this factor is of limited value, when interpore distance is kept at a constant instead of being variable. In addition to this it was also observed that the pore could be widened if the anodization basic parameters are changed based on pore widening route.

In this research, $TiO_2$ nanorods were fruitfully grown inside the channels of (AAO) porous anodic aluminium oxide templates at near ambience by the electrochemical deposition method. A direct current (DC) electric field was used to fill the template pores with the titanium powder emulsion. Very stabilized titanium sols were prepared during chemical modification of titanium powder in the company of oxalic acid. Nanorods of diameters of 25–93 nm have been effectively grown. Crystallites of $TiO_2$ nanorods are larger than those of $TiO_2$ powder. SEM micrographs indicate the appropriateness of the direct current (DC) electrolysis as a successful method to fill the aluminium oxide templates with $TiO_2$ precursor material. $TiO_2$ nanorods in close-packed arrays were formed after heat curing of the filled templates. The AAO template process is an all-purpose way of getting organic nanorods, nanotubes, or nanowires of the required aspect ratio that ranged from 7 nm to 400 nm. These unique templates may also be used to produce small molecules of a one-dimensional nature. Hence, we emphasize that this method developed for the template-based synthesis of $TiO_2$ nanorods is quite appropriate, cost effective, and gives densely packed ordered nanorods and overcomes the limitations of other synthetic methods.

## REFERENCES


1. D.W. Bahnemann, M. Hilgendorff, and R. Memming, *J. Phys. Chem. B* 101, 4265 (1997).
2. H.C. Zeng, in *The Dekker Encyclopedia of Nanoscience and Nanotechnology*. (Marcel Dekker, New York, 2004), pp. 2539–2550.
3. C.L. Olson, J. Nelson, and M.S. Islam, *J. Phys. Chem. B* 110, 9995 (2006).
4. L. Xeubing and E. Iglesia, *Angew. Chem. Int. Ed. Engl.* 46, 8649 (2007).
5. A. Furube, L. Du, K. Hara, R. Katoh, and M. Tachiya, *J. Am. Chem. Soc.* 129, 14852 (2007).
6. J. Nowotny, T. Bak, M.K. Nowtny, and L.R. Sheppard, *Int. J. Hydrog. Energy* 32, 2630 (2007).
7. M.K. Nowotny, L.R. Sheppard, T. Bak, and J. Nowotny, *J. Phys. Chem C.* 112, 5275 (2008).
8. A.L. Linsebigle, R.L. Guangquan, and J.T. Yates, *Chem. Rev.* 95, 735 (1995).
9. P.V. Kamat, *Chem. Rev.* 93, 267 (1993).
10. P. Roy, S. Berger, and P. Schmuki, *Angew. Chem. Int. Ed. Engl.* 50, 2904 (2011).
11. C. Su, B.Y. Hong, and C.M. Tseng, *Catal. Today* 96, 119 (2004).
12. H.J. Yun, H. Lee, J.B. Joo, W. Kim, and J. Yi, *J. Phys. Chem. C* 113, 3050 (2009).
13. R. Beranek, H. Hildebrand, and P. Schmuki, *Elecrochem. Solid state lett.* 6, B12 (2003).
14. O.K. Varghese, D. Gong, M. Paulose, K.G. Ong, E.C. Dickey, and C.A. Grimes, *J. Adv. Mater.* 15, 624 (2003).
15. E.M. Guerrra and M. Mulato, *Mater. Sci. Appl.* 5, 459 (2014).
16. R. Clarke, R. Hill, and D.R. Roberts, *J. Chem. Technol. Biotechnol.* 68, 397 (1997).
17. A. Birner, R. Wehrspohn, U.G. Sele, and K. Busch, *J. Adv. Mater.* 13, 377 (2001).
18. C. Haginoya, M. Ishibashi, and K. Koike, *Appl. Phys. Lett.* 71, 2934 (1997).
19. H. Masuda, M. Yotsuya, M. Asano, K. Nishio, M. Nakano, A. Yokoo, and T. Tamamura, *Appl. Phys. Lett.* 78, 828 (2001).
20. H. Imai, Y. Takei, K. Shimizu, M. Matsuda, and H. Hirashima, *J. Mater. Chem.* 9, 2971 (1999).
21. P. Hoyer, *J. Adv. Mater.* 8, 857 (2004).
22. Z. Miao, D. Xu, J. Ouyang, G. Guo, X. Zhao, and Y. Tang, *Nano Lett.* 2, 717 (2002).
23. D. Gong, C.A. Grimes, O.K. Varghese, W. Hu, R.S. Singh, Z. Chen, and E.C. Dickey, *J. Mater. Res.* 16, 3331 (2001).
24. O. Jessensky, F. Muller, and U. Gosele, *Appl. Phys. Lett.* 72, 1173 (1998).
25. C.R. Martin, *Chem. Mater.* 8, 1739 (1996).
26. J.C. Hulteen and C.R. Marter, *J. Mater. Chem.* 7, 1075 (1997).
27. E.J.P. Gerrard, A. Nurshahidah, and F. Derek, *Materials* 4, 487 (2011).
28. A. Nourmohammadi, M. Mehrjuee, and M.A. Bahrevar, *IJE. Trans. B: Appl.* 25, 343 (2012).
29. M.R. Mohammadi, F. Ordikhani, D.J. Fray, and F. Khomamizadeh, *Particuology* 9, 161–169 (2011).
30. M.A. Kashi and A. Ramazani, *Int. J. Nanosci. Nanotechnol.* 6, 78 (2010).
31. G.E. Thompson, Y. Xu, P. Skeldon, K. Shimizu, S.H. Han, and G.C. Wood, *Philos. Mag. B* 55, 651 (1987).
32. S.J. Garcia-Vergarai, L. Iglesias-Rubianes, C.E. Blanco-Pinzon, P. Skeldon, G.E. Thompson, and P. Campestrini, *Proc. R. Soc. Lond. A.* 462, 2345 (2006).
33. L. Feiyue, L. Zhang, and R.M. Metzger, *Chem. Mater.* 10, 2470 (1998).
34. S. Xu and Z.L. Wang, *Nano Res.* 4, 1013 (2011).